Moisture Transfer in Roof Sections Under Cyclic Conditions and Constant Air Pressure Difference—Laboratory and Modelling Studies

M. J. CUNNINGHAM*

The predictions of a finite-difference moisture transfer model SMAHT (Simulation of Moisture And Heat Transfer) are compared to data obtained from laboratory studies on the drying of timber members and plywood components of 1 metre square roof sections subjected over 50 days to cyclic temperature and humidity conditions and constant air pressure difference. The numerical model accurately predicted the moisture performance of these structures, except for the one case when condensation was about to form within the structure. In this case the model prediction for asymptotic moisture content was 5% moisture content too low. A simple analytical model based on mean driving force values also gave good results, except in the close-to-condensing case.

INTRODUCTION

IT IS WIDELY accepted that an important route towards an understanding of the moisture performance of structures is via mathematical modelling of these systems [1]. Several numerical models exist for moisture transfer in structures [2–11] of various degrees of sophistication and various degrees of validation and comparison with experimental results. Of these, perhaps WALLDRY [7] is the model most thoroughly compared to field results.

In earlier work [10, 11], the author described a finite-difference nodal model, now named SMAHT (Simulation of Moisture And Heat Transfer), and reported some preliminary work in comparing the model predictions against experimental data. However, the experiments carried out for the earlier study, [12], were of a rather simplified nature. Roof sections were designed to have low air-leakage and were subjected to constant driving forces of temperature and humidity. For more confidence in the ability of the model to predict accurately moisture performance of structures, firstly time varying temperature and relative humidity driving forces are needed, and secondly experiments need to be carried out upon specimens with realistic air-leakage properties.

An analytical model developed by the author, [13], gives certain indications as to what might be expected under these conditions. This model puts vapour diffusion and air leakage on an equal footing, predicting that specimens with significant air leakage should behave only quantitatively and not qualitatively differently from tighter specimens. This same model states that the moisture performance of the structure under cyclic conditions

can be predicted approximately by considering only the mean values of the cyclic driving forces. Neither remark above can be expected to be true under conditions where condensation is likely to take place.

This work reports the outcome of carrying out experiments under cyclic conditions with constant air pressure difference and comparing the predictions of the numerical model SMAHT to this experimental data.

EXPERIMENTAL DETAILS

Four 1-metre square roof section specimens with wet timber members were placed between controlled climate chambers and allowed to dry over a period of 50 days under conditions of periodic driving forces and constant air pressure difference, see Fig. 1. Temperature and relative humidity were separately controlled above and below the specimen. Moisture content, relative humidity, temperatures and condensation were measured and logged automatically.

In detail, two specimen types were used, see Fig. 2. Specimens 1 and 2 were concrete tiled specimens separated from a ceiling by 25×50 mm tile battens and a $50 \times 50 \times 950$ mm rafter, see Fig. 2(a). Building paper was laid over the rafter, and 75 mm fibre-glass batt insulation squashed under this to a compressed height of 50 mm (as is common building practice in New Zealand for this kind of roof. Note also that this kind of roof would normally be supported on external exposed rafters). Specimens 3 and 4 consisted of a rubber membrane on plywood roof separated from a ceiling by a $140 \times 45 \times 950$ mm joint, see Fig. 2(b). 75 mm fibre-glass batt insulation was placed in the cavity. Specimens 1 and 4 had unpainted foil-backed gypsum plasterboard ceilings; specimens 2 and 3 had ceilings made of factory primed woodfibre tiles, 300 mm square. Details of specimen edge

* Building Physicist, BRANZ, Moonshine Road, Judgeford, Private Bag 50908 Porirua, New Zealand.
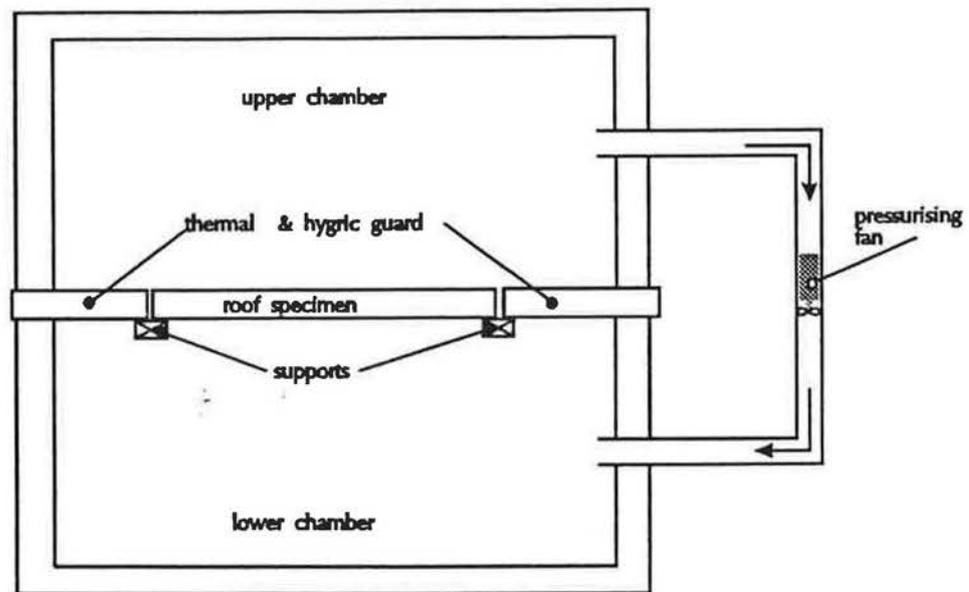
Fig. 1.Schematic diagram of specimen and controlled climate chambers.

detailing to minimize lateral heat and moisture flows are given in [12].

The rafter of the first specimen type and the joist of the second type were presoaked for 7 or 8 days, placed into the specimen, and the ceiling attached. The air-tightness of the specimen was then found by measuring the air flow rate through the specimen for a given air pressure difference applied across it using a special rig, see [12], and the specimen then placed between the two controlled climate chambers.

Each specimen was subjected to constant air pressure difference, nominally of 20 Pa, the indoor side of the specimen being at the higher pressure. This pressure difference was maintained by a fan system ducting air from the upper climate chamber to the lower climate chamber. This air pressure difference was monitored and logged along with the other parameters mentioned below. The air leakage through the cavity of each specimen was calculated from the measured air-tightness and the air

pressure differences measured across the specimen in place between the chambers. These values are contained in Table 1.

Each specimen was subjected to a varying temperature and relative humidity regime chosen to approximate the range of indoor and outdoor conditions found in New Zealand winters. The upper chamber was controlled to a sol-air temperature value, with the relative humidity being adjusted to give the water vapour pressures experienced at ambient air temperatures e.g. if the ambient conditions to be simulated were 20°C and 70% RH, and the sol-air temperature to be simulated was 25°C, then the top chamber was set to 25°C and 51% RH, which gives 1650 Pa vapour pressure in both cases. The lower chamber had a small amplitude diurnal temperature variation, with the relative humidity adjusted to give a constant vapour pressure. Temperature and humidity in the bottom chamber were varied sinusoidally with a 24 hour period. The upper chamber driving forces were also

Table 1. Envelope details and driving forces for each specimen

	Specimen number			
	1	2	3	4
Roof cladding	Concrete tiles	Concrete tiles	Rubber membrane on plywood	Rubber membrane on plywood
Ceiling lining	Foil backed gypsum plasterboard	Woodfibre tiles	Woodfibre tiles	Foil backed gypsum plasterboard
Air leakage (hr^{-1})	0.08	2.15	1.26	0.11
Top chamber mean temperature	12.2°C	7.7°C	11.8°C	6.7°C
Top chamber temperature amplitude	11.8°C	8.9°C	11.2°C	8.8°C
Top chamber nominal mean RH	85%	81%	85%	80%
Top chamber RH nominal amplitude*	38%	38%	38%	34%
Top chamber max RH	87%	81%	95%	80%
Bottom chamber mean temperature	19.3°C	19.7°C	19.6°C	18.0°C
Bottom chamber temperature amplitude	1.8°C	1.0°C	1.3°C	1.6°C
Bottom chamber vapour pressure	1150 Pa	1150 Pa	1400 Pa	1400 Pa

* Clipped, see Fig. 3.
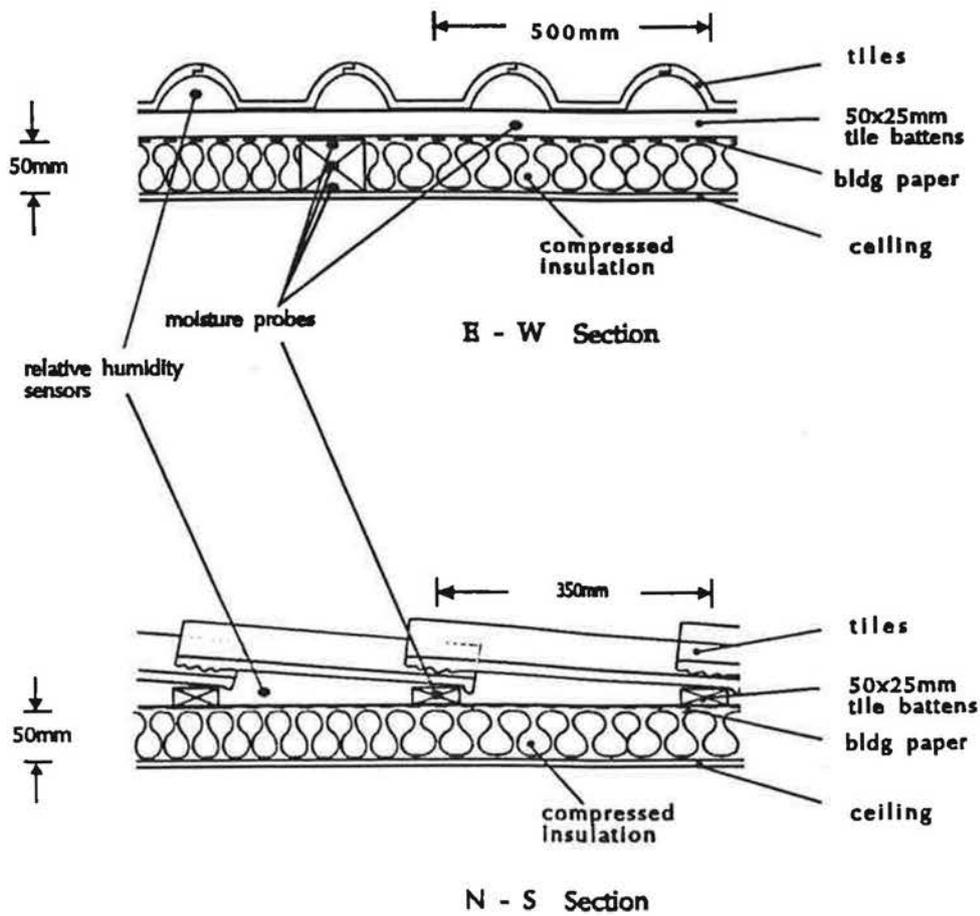
2(a): Cross sections of the first specimen type
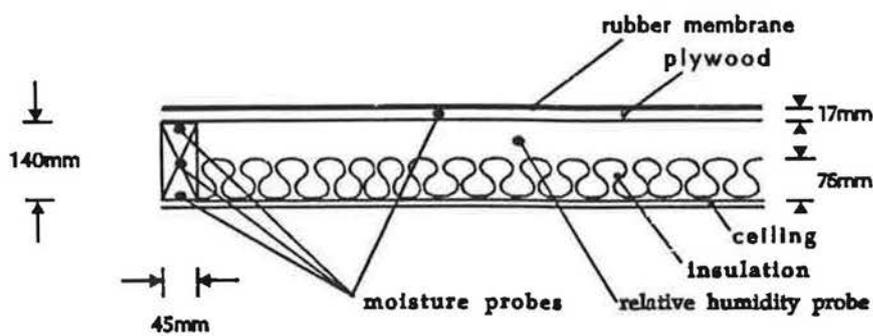
2(b): Cross section of the second specimen type

Fig. 2. Specimen cross sections.

nominally sinusoidal with a 24 hour period, but with the relative humidity being limited to a maximum value. In practice, this means that in some cases only the lower half of the sinusoid is present in the relative humidity time profile, and for the second half of the period the relative humidity is clipped at its maximum value. This clipping is illustrated in Fig. 3 which shows a typical 3 day record for the driving forces for specimen 4. Table 1 shows the details of the driving forces as measured by the datalogging equipment, with the term "nominal mean RH" being used for the top chamber relative humidity to indicate the mean relative humidity that would have existed had there been no clipping.

Each specimen had four timber moisture probes of a resistive type described elsewhere, [14], with associated thermocouples, and a capacitive relative humidity sensor placed in the specimen air cavity, also with associated thermocouples. Figure 2 shows the location of these transducers.

A condensation probe was placed on the building paper of specimens 1 and 2 and on the cavity surface of the plywood of specimens 3 and 4. In the case of specimens 1 and 2, this probe consisted of two 2 mm diameter screws acting as electrodes bolted through the building paper, with the screw axes being 14 mm apart. In the case of specimens 3 and 4, this probe consisted of two 30 mm long parallel strips of conducting paint painted on the plywood, with the inside edges of the strip being 5 mm apart. The resistance between the electrodes of these

probes provides an indication of the presence of condensation.

The experimental uncertainties due to these transducers are estimated to be : for the moisture probes $\pm 1\%$ moisture content at 15% moisture content, rising to $\pm 5\%$ moisture content at 30% moisture content, see [14]; for the relative humidity sensor $\pm 5\%$ RH; for the thermocouples $\pm 0.2°C$. The condensation probe is qualitative only.

A computer datalogging system was used to measure and log the moisture content every two hours and the relative humidity, temperature and condensation probes every quarter of an hour.

EXPERIMENTAL RESULTS

Figure 4 shows the individual daily mean moisture contents measured at each moisture probe for each specimen (Fig. 4(b) does not show the experimental results for the probe in the lower part of the rafter, as this probe failed early in the run). Figure 5 shows the mean moisture content for the rafter of specimens 1 and 2 and the plywood for specimens 3 and 4. Included with Fig. 5 are model predictions discussed in the next section. The mean was calculated by volume weighting the moisture contents for individual probes. Plywood was chosen for closer investigation in specimens 3 and 4 because for these specimens it represents a larger volume of wood
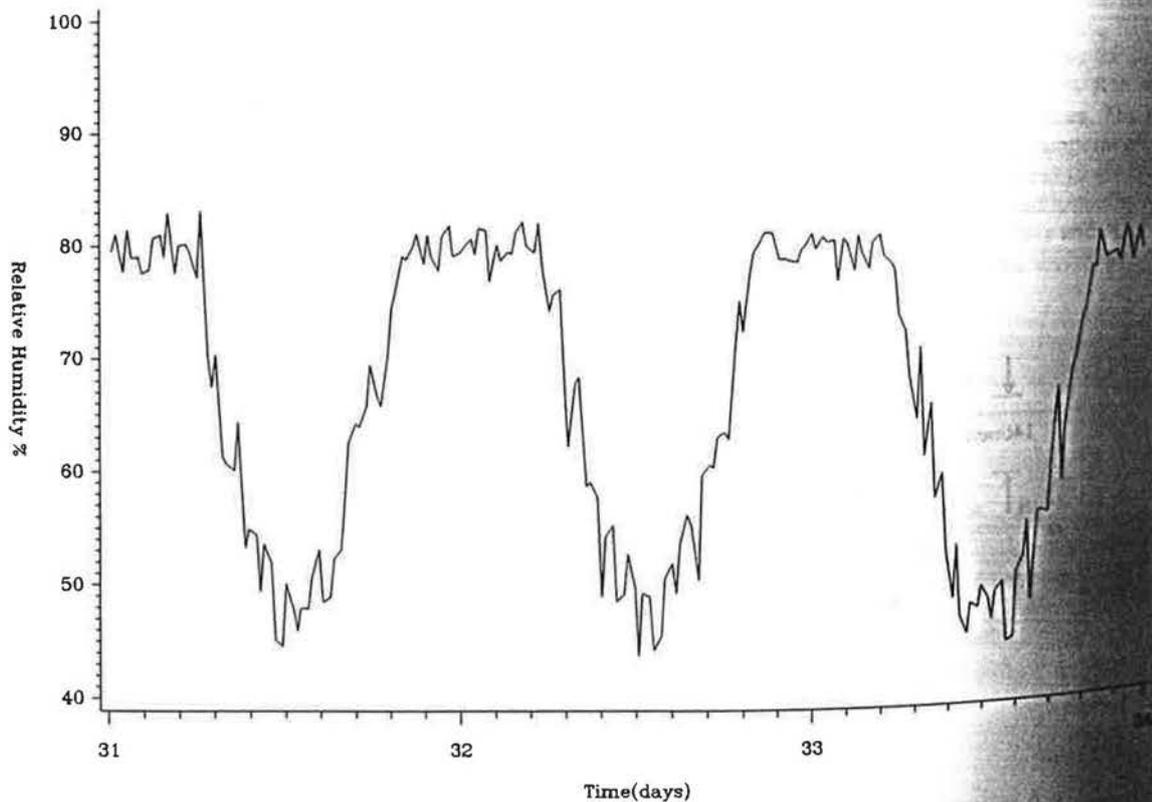
Fig. 3. Typical upper chamber relative humidity driving force (specimen 4) showing clipping at high relative humidities.
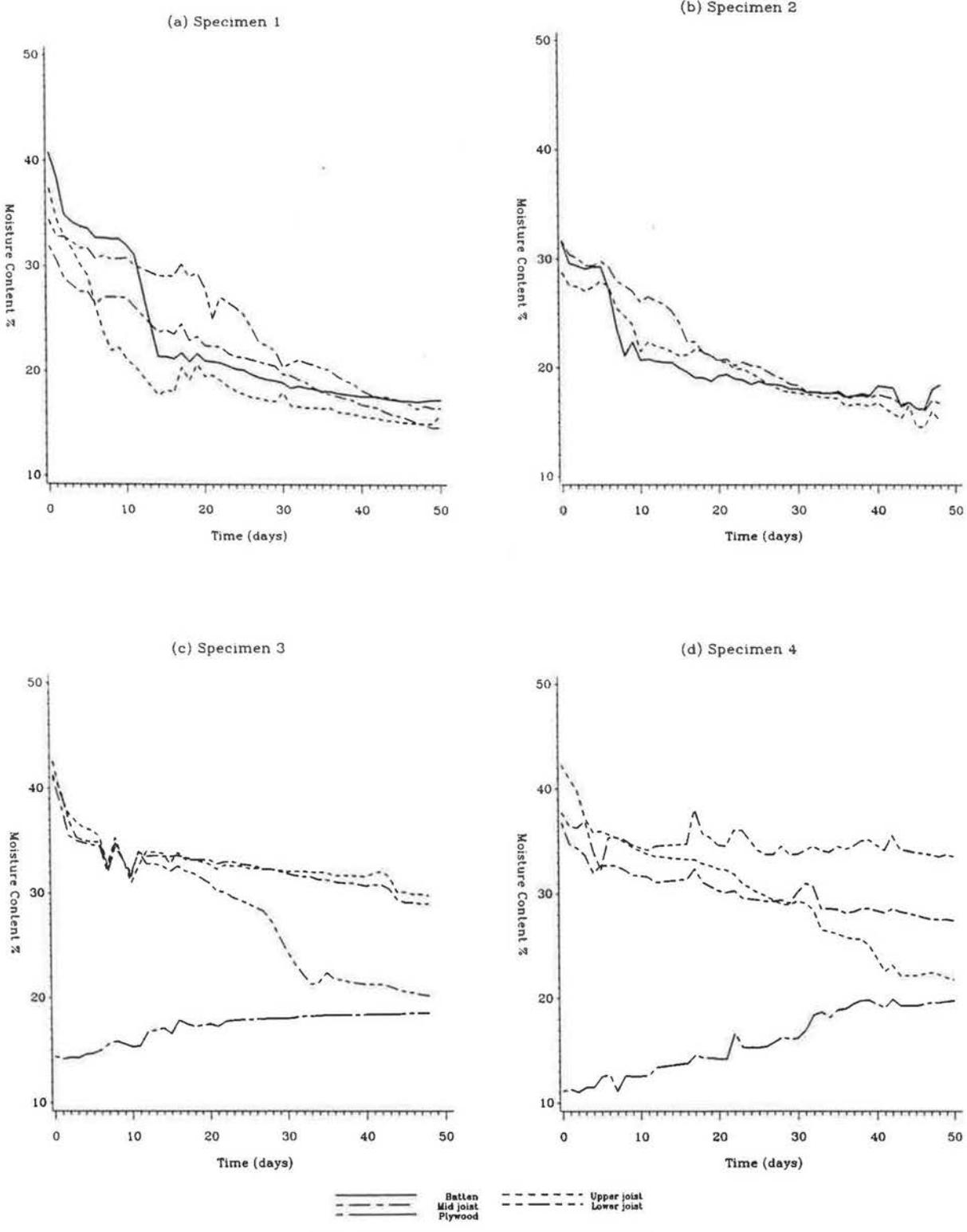
Fig. 4. Specimen experimental moisture contents.

M. J. Cunningham
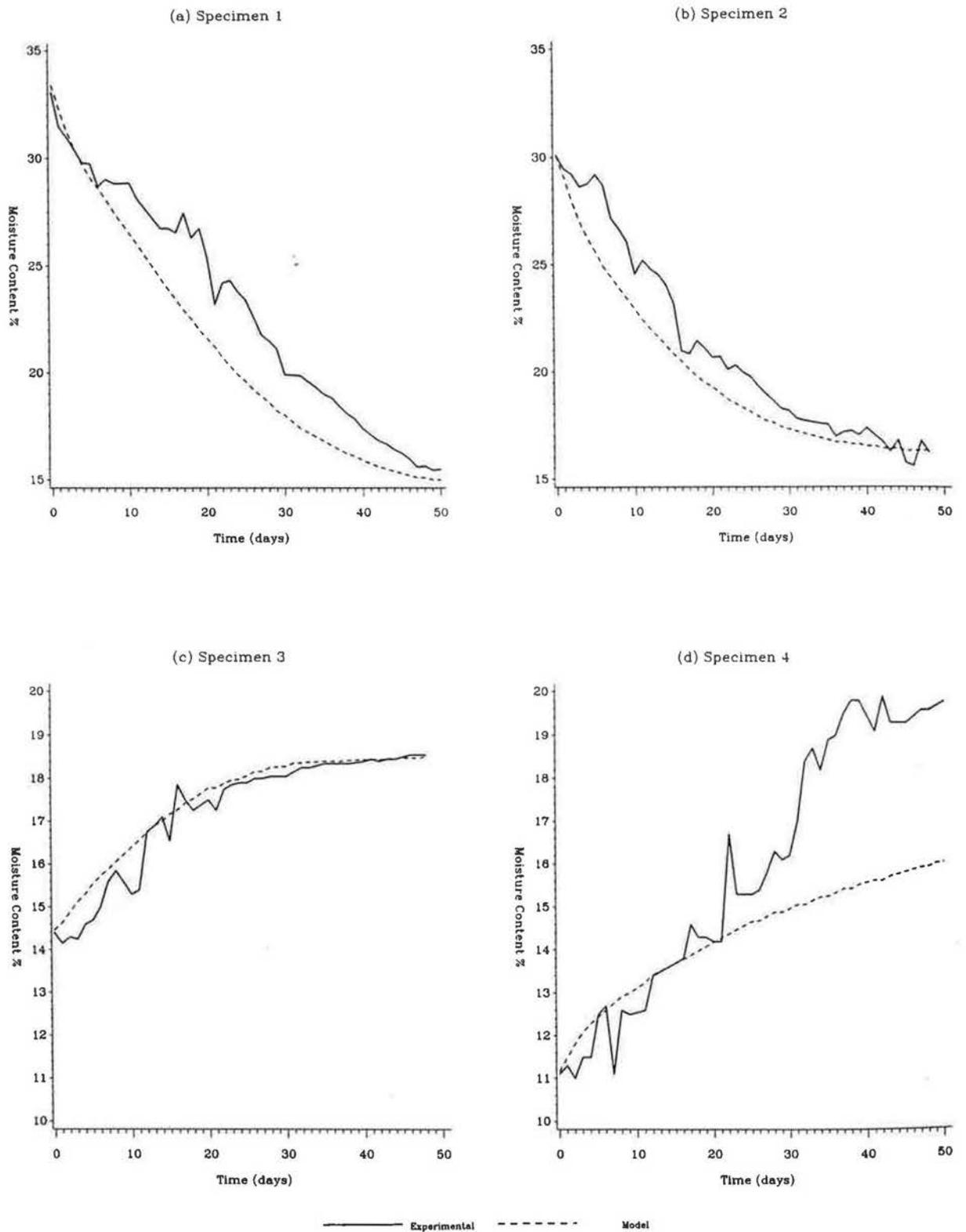
Fig. 5. Experimental and model-predicted mean moisture contents. Specimens 1 and 2, rafter moisture content; specimens 3 and 4, plywood moisture contents.

Table 2. Experimental and model results for asymptotic moisture contents and time constants for each specimen

Specimen number	Component	Quantity	Experimental	Results Numerical	Analytical
1	Rafter	Asymptote	13.0%	13.0%	14.0%
		Time constant	33 days	32 days	20 days
2	Rafter	Asymptote	15.0%	15.5%	16.5%
		Time constant	19 days	15 days	15 days
3	Plywood	Asymptote	18.5%	18.5%	18.0%
		Time constant	15 days	12.5 days	12.5 days
4	Plywood	Asymptote	23.0%	18.0%	27.0%
		Time constant	33 days	33 days	113 days

and has a larger surface area exposed to the cavity than the joist.

From the experimental results an asymptotic moisture content and an exponential time constant were calculated. This calculation was done by taking all results below fibre-saturation (30% moisture content) and fitting an exponential curve to the data. These results are contained in Table 2.

Drying time constant and asymptotic moisture content are the two key parameters to the moisture performance of a drying specimen. Indeed, Cunningham has shown [13, 15] that these parameters are sufficient to describe the moisture performance of a structure under any conditions, in so far as the set of differential equations describing the physics of moisture performance of a structure are linear.

Only in the case of specimen 4 was significant condensation measured, and even in that case it was only intermittent. The output of the condensation probe for specimen 4 over 4 days is shown in Fig. 6. In this graph, the vertical axis is the measured resistance of the moisture probe. Separate calibration trials showed that the dip to 1 Mohm resistance represents a small amount of condensation which quickly dries out as the temperature rises.
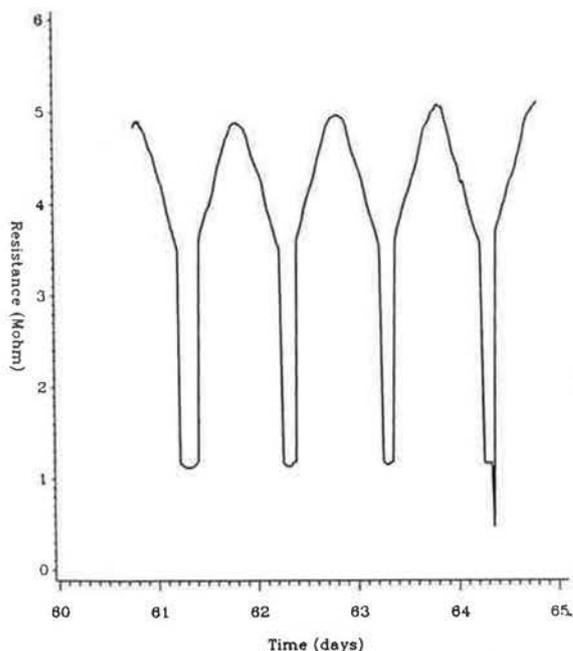
The experimental results found are understandable in terms of the mean value of the driving forces above and below the specimen, and the vapour- and air-tightness of the specimen. Indeed, the analytical model merely serves to place this intuitive understanding on a formal basis. In detail—

Specimen 1 is vapour- and air-tight from the ceiling to the building paper, and is driven by a lower vapour pressure from below and a warmer temperature from above. As a consequence, the rafter has the lowest asymptotic moisture content at 13% but, being tight, it has a long time constant at 33 days.

Specimen 2 is vapour- and air-loose, is driven by a lower vapour pressure from below and a lower temperature from above. As a consequence, it has a slightly higher asymptotic moisture content than specimen 1 at 15% but, being loose, it has a much shorter time constant at 19 days.

Specimen 3 has a roof cladding which is vapour- and air-tight but a ceiling which is vapour- and air-loose. It is driven by a higher vapour pressure from below and a warmer temperature from above. The ease of access of moisture from below into the specimen causes the plywood asymptotic moisture content to be moderately high at 18.5% but the relatively warm roof temperatures prevent the moisture content from rising above this. Because the ceiling is relatively loose, the time constant is shorter at 15 days.

Specimen 4 is vapour- and air-tight, is driven by a higher vapour pressure from below and a lower temperature from above. Consequently, this specimen is close to forming condensation in the plywood. Indeed, elementary calculations, and also the analytical model predict that condensation should accumulate on the cold plywood. However, both the experimental results and the numerical model show that condensation is only intermittent due to absorption by the plywood. Because the specimen is tight, it has a long time constant at 33 days.

MODEL COMPARISONS

The experimental results were compared to predictions using the numerical model described previously [8, 9].

Fig. 6. Specimen 4 condensation probe output.

(a) First specimen type

(b) Second specimen type
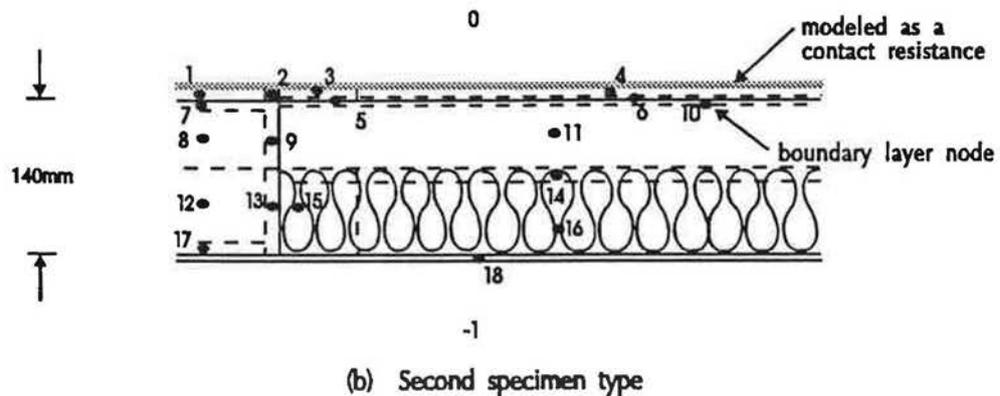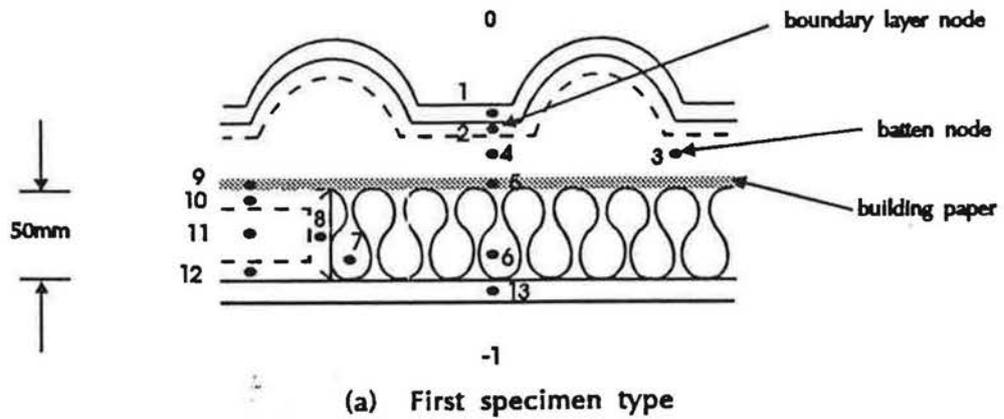
Fig. 7. Nodal structure of specimens.

SMAHT is a finite-difference nodal model, where the positions of the nodes are free to be chosen according to the needs of the user. Figure 7 shows the nodal positions used for the purposes of this work. Specimens 3 and 4 are modelled 2-dimensionally, but specimens 1 and 2 have a 3-dimensional factor, in that the tile batten runs at right angles to the main rafter and has a dimension of 50 mm in the third dimension whereas all other components have a length of 950 mm in this third dimension.

Table 3 contains the values of diffusion coefficient and thermal conductivity used for the various materials making up the specimens. As was done in the earlier study, [11], above fibre saturation an effective vapour diffusion coefficient was used. Correct mass transfer rates are not

well known at these moisture contents [16], and in the context of the durability of structures, one would require that moisture contents were not at these levels for long periods of time. Figure 8 shows the vapour diffusion coefficient chosen for the timber as a function of moisture content. As earlier, this variation in the diffusion coefficient above fibre saturation has been chosen merely to give good agreement with results above fibre saturation, and as such is the least satisfactory aspect of

Table 3. Values used for material coefficients

Material	Vapour diffusion coefficient s	Thermal conductivity $W\,m^{-1}\,^\circ C^{-1}$
Wood	1.0×10^{-11}	0.18
Woodfibre board	0.9×10^{-11}	0.054
Plywood	1.4×10^{-11}	0.12
Plasterboard	3.0×10^{-11}	0.22
Fibreglass batts	2.0×10^{-10}	0.05
Concrete tiles	1.1×10^{-11}	1.0
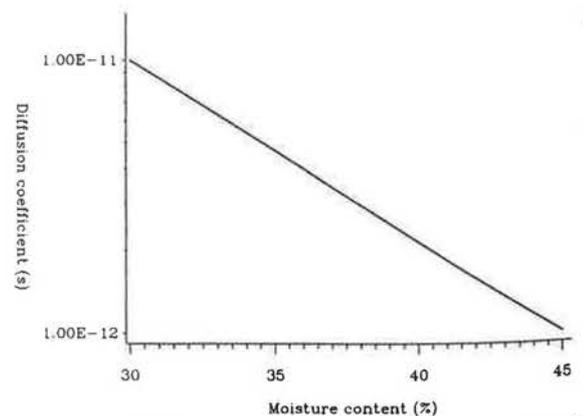
Fig. 8. Effective diffusion coefficient above fibre-saturation used in the model.

the modelling described here; however, the present state of knowledge makes this kind of approach inevitable.

Sorption data obtained by Cunningham and Sprott, [17], is used to describe the hygroscopic properties of the materials.

The vapour resistances of the rubber membrane roof cladding and the foil of the foil-backed plasterboard ceiling were taken as 100 and 10 $GNskg^{-1}$ respectively. Model predictions are insensitive to the exact values used as air leakage tends to dominate when linings are this tight.

Figure 5 shows the model predictions and experimental results for the mean moisture content for the rafter of specimens 1 and 2 and the plywood for specimens 3 and 4. Table 2 contains the asymptotic moisture contents and time constants calculated from the model predictions.

Included in Table 2 are analytical model predictions. This model has been extensively discussed elsewhere, [11, 15]. In essence, the asymptotic moisture content is calculated by considering the result on the rafter or plywood moisture contents of a weighted average of the mean value of the driving forces, and the time constant is calculated by considering the inhibition to drying caused by the moisture flow resistances of the linings.

As can be seen in Fig. 5 and Table 2, for specimens 1, 2 and 3 the agreement between the numerical model and the experimental results is very good, with the asymptotic moisture contents being predicted to within 0.5% moisture content and the time constants to within 4 days. Agreement is not so good for the case of specimen 4. Here, although the time constant prediction is identical to that observed, the numerical model predicts an asymptotic value of 18% moisture content compared to the experimental result of 23%. This was a difficult case to predict because the specimen was undergoing intermittent condensation. Consequently, capillary absorption into the plywood is an important mechanism which, as has been explained above, is not well handled by this model, due chiefly to an inadequate knowledge of the size of the diffusion coefficients. Furthermore, both the specimen and model performance are very sensitive to small changes in the value of the driving parameters, particularly the temperature of the upper chamber. The numerical model predicts intermittent condensation in this case, and this is borne out experimentally, see Fig. 6.

The difficulty in predicting moisture performance when a structure is close to forming condensation was highlighted by the fact that in initial modelling only one layer was used to model the plywood. Model predictions in this case showed a continuous build-up in condensation because the single plywood layer was too resistant to diffusion to allow for rapid absorption of the condensate.

The secondary parameter of relative humidity was not as well predicted as the primary parameter of moisture content. Figure 9 shows a typical daily cycle of relative humidity measured in the cavity of specimen 1, 38 days after the commencement of the run. Also shown is the predicted result. The predicted result is 9% RH too high and tends to lead the experimental result for the first part of the cycle by a few hours. On the other hand the predicted and experimental amplitudes are the same. This tendency to predict too high was a general one and is
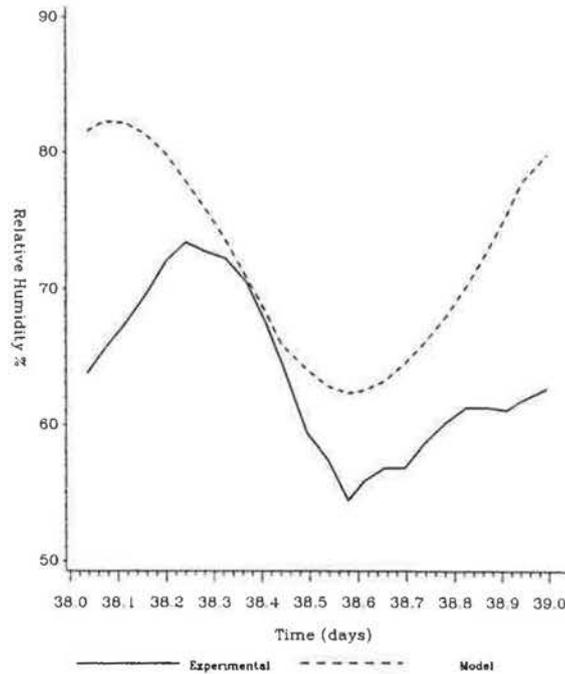
Fig. 9. Specimen 1 experimental and model-predicted relative humidity.

difficult to explain. Part of the answer may be experimental—temperature gradients within the cavity of the specimens give rise to relative humidity gradients so that a small shift in the vertical position of the relative humidity sensor will change its observed value. Also, rather small differences in model cavity temperature predictions created by small changes in the value of thermal conductivity of the components of the specimens give rise to different relative humidity predictions.

The analytical model gives moderately accurate agreement with the experimental results, except again for specimen 4. Here the analytical model predicts that condensation will take place on the plywood—the analytical model prediction for the asymptotic moisture content for the plywood has been rather arbitrarily set to the fibresaturation value of 27%. The time constant prediction is poor (113 days versus the experimental result of 33 days). These results highlight the fact that when a structure is close to condensation its exact behaviour becomes somewhat difficult to predict accurately.

Specimen 4 predictions aside, the performance of the analytical model is quite good when it is remembered that it deals with mean conditions only and does not consider moisture and temperature gradients. Perhaps the results are not so surprising when one considers the fact that the author has shown, see [18], that under some circumstances, lumped modelling gives results identical to that predicted by exact solutions of the underlying mass transfer differential equations.

CONCLUSIONS

The model comparison studies have confirmed that the numerical model SMAHT can predict moisture contents well except when a structure is close to forming con-

densation. In this case the model predicted the correct time constant for drying of the plywood, but predicted an asymptotic moisture content value that was 5% moisture content too low. When condensation is close to forming, very small changes in driving forces will drastically change a structure's performance, so it is not surprising that the model reflects the uncertainty of outcome in the physical world caused by this sensitivity to small change.

Simpler modelling via an analytical model also gives good results except in the close-to-condensing case, emphasising that such an approach can be quite useful, and gives predictions which are far more than merely qualitative.

It remains to trial the model against field data which is a much more testing situation, experimentally as well as from the modelling point of view. This work is currently being undertaken, and will allow the performance of SMAHT to be checked when a number of issues come into play that cannot be easily simulated in the laboratory. These issues include physical mechanisms like cross ventilation and night sky radiation, and other factors such as speed of construction and occupant behaviour.

REFERENCES

1. *National Program Plan Building Thermal Envelope*. Third Edition. Building Thermal Envelope Co-ordinating Council (1988).
2. A. Tenwolde, The Kieper and MOISTWALL analysis methods for walls. *Proc. ASHRAE/DOE conference, Thermal Performance of the Exterior Envelope of Buildings* II, p. 1033 (1982).
3. D. M. Burch and D. E. Luna, A mathematical model for predicting attic ventilation rates required for the prevention of condensation in roof sheathing. *ASHRAE Trans*, part 1, 201 (1980).
4. P. Cleary and R. Sonderegger, A method to predict the hour by hour humidity ratio of attic air. *ASTM Symposium on Thermal Insulation, Materials and Systems*, Dallas (1984).
5. R. Kohonen, Transient Analysis of the Thermal and Moisture Physical Behaviour of Building Constructions, *Bldg Envir*. **19**, 1–11 (1984).
6. A. A. Kerestecioglu, L. Gu, Theoretical and computational investigation of simultaneous heat and moisture transfer in buildings: "evaporation and condensation" theory, *ASHRAE Trans*, **96**, part 1, 455 (1990).
7. G. K. Yuill and Assocs, Comparison of WALLDRY predictions with Atlantic Canada moisture test hut data, Canada Mortgage and Housing Corporation, Ottawa (1990).
8. C. R. Pedersen, Combined heat and moisture transfer in building constructions Report No. 214, Technical University of Denmark, Thermal Insulation Laboratory, Lyngby (1990).
9. D. M. Burch and W. C. Thomas, An analysis of moisture accumulation in a wood frame wall subjected to winter climate. NISTIR 4674 National Institute of Standards and Technology, Gaithersburg, Maryland (1991).
10. M. J. Cunningham, Modelling of moisture transfer in structures—I. A description of a finite-difference nodal model. *Bldg Envir*. **25**, 55–61 (1990).
11. M. J. Cunningham, Modelling of moisture transfer in structures—II. A comparison of a numerical model, an analytical model and some experimental results. *Bldg Envir*. **25**, 85–94 (1990).
12. M. J. Cunningham, Drying of construction moisture in timber framed flat roofs. I. Low air leakage. *ASHRAE Trans*. **93**, part 2, 153–170 (1987).
13. M. J. Cunningham, The Moisture Performance of Framed Structures—A Mathematical Model. *Bldg Envir*. **23**, 123–125 (1988).
14. M. J. Cunningham, Automatic datalogging timber moisture contents over the range 10%–50% w/w. *ISA Trans*. **25**, No. 3, 73–80 (1986).
15. M. J. Cunningham, Further analytical studies of building cavity moisture concentrations. *Bldg Envir*. **19**, 21–29 (1984).
16. M. J. Cunningham, Isothermal moisture transfer coefficients in Pinus radiata above the fibre-saturation point using the moment method. *Wood and Fiber Science* **21**, 112–122 (1989).
17. M. J. Cunningham and T. J. Sprott, Sorption properties of New Zealand building materials. Research report R43, Building Research Association of New Zealand, Judgeford (1984).
18. M. J. Cunningham, Effective penetration depth and effective resistance in moisture transfer. *Bldg Envir*. **27**, 379–386 (1992).